# Two-Dimensional Electronic Spectroscopy unravels sub-100-fs Electron and Hole Relaxation Dynamics in Cd-Chalcogenide Nanostructures

*Tatjana Stoll[1], Federico Branchi[1], Julien Rehault[1], Francesco Scotognella[1,2], Francesco Tassone[2], Ilka Kriegel[3,4]\* and Giulio Cerullo[1]\**

[1] IFN-CNR, Dipartimento di Fisica, Politecnico di Milano, Piazza L. da Vinci 32, 20133 Milano, Italy

[2] Center for Nano Science and Technology CNST-IIT@PoliMi, Istituto Italiano di Tecnologia, via Pascoli 70/3, 20133 Milano, Italy

[3] Department of Nanochemistry, Instituto Italiano di Tecnologia (IIT), via Morego, 30, 16163 Genova, Italy

[4] Molecular Foundry Lawrence Berkeley National Laboratory, Berkeley, CA 94720, USA

## Experimental setup

Two-Dimensional Electron Spectroscopy (2DES) is the most advanced ultrafast spectroscopy technique, which combines ultrahigh temporal and spectral resolution in both excitation and detection. The partially collinear pump-probe geometry used for these measurements and shown schematically in Figure S1, can be seen as an extension of conventional transient absorption spectroscopy, where two identical pump pulses are used and their delay $t_1$ (coherence time) is scanned in time, for a given value of the population or waiting time $t_2$. The probe pulse is dispersed in a spectrometer, providing resolution on the detection frequency, while the Fourier transform of the nonlinear signal with respect to the pump pulses delay $t_1$ provides the resolution on the excitation frequency[1,2,3].
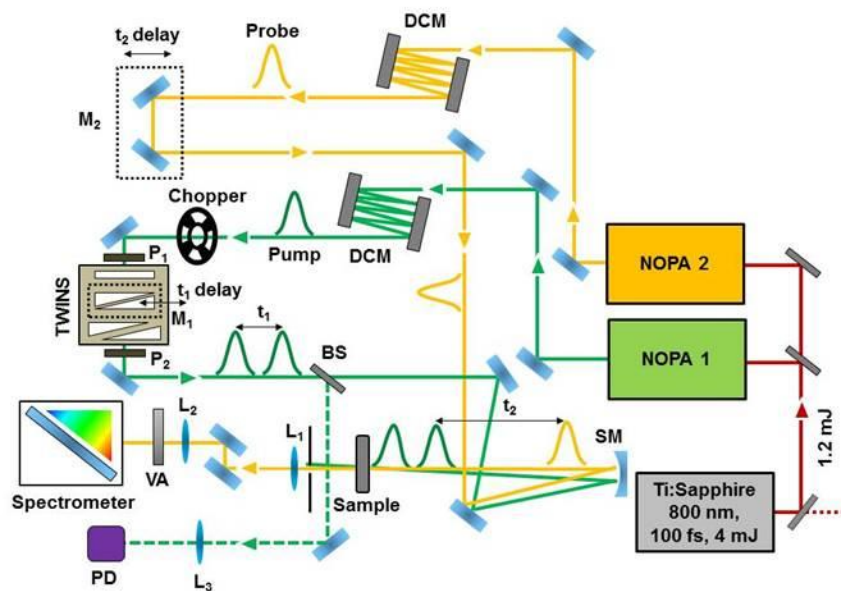


**Figure S1.** Set-up for femtosecond 2DES. NOPA: non-collinear optical parametric amplifier; DCM: double chirped mirror; PD: photodiode; L: converging lens; $t_1$: linear translation for pump pulse pair delay; $t_2$: linear translation for pump-probe delay; BS: beam splitter; P: polarizer

number; M: motorized delay; TWINS: Translating-Wedge-Based Identical Pulses eNcoding System; VA: variable pulse attenuator; SM: spherical mirror.

Our 2DES setup is built around a commercially amplified Ti:sapphire laser system (Libra, Coherent) delivering 4-mJ, 100-fs pulses at 800 nm, and 1-kHz repetition rate. Portions of the laser with 300 μJ energy respectively are used to pump two synchronized, non-collinear optical amplifiers (NOPAs) generating the pump and probe pulses. Both NOPAs deliver visible pulses with a spectrum tunable between 2.4 eV and 1.6 eV. They are compressed to sub-10-fs duration by multiple bounces on custom-designed double-chirped mirrors (DCMs), measured by the frequency-resolved optical gating (FROG) technique[4]. The phase-locked pair of femtosecond pump pulses is generated by the Translating-Wedge-Based Identical-Pulses-eNcoding System (TWINS) technology[5,6]. TWINS exploits birefringence to impose user-controlled temporal delays, with attosecond precision, between two orthogonal components of broad-bandwidth laser pulses. Rapid scanning of the inter-pulse delay $t_1$ allows robust and reliable generation of 2DES maps, for in a user-friendly pump-probe geometry. Portion of the pump beam is split off and sent to a photodiode to monitor the interferogram of the pump pulse pair, in order to determine zero delay between the pulses and properly phase the 2DES spectra The dispersion introduced by the TWINS on the pump pulse pair is compensated by a suitable number of bounces on a pair of DCMs, and spectral phase correction is checked using a Spatially Encoded Arrangement for Temporal Analysis by Dispersing a Pair Of Light E-fields (SEA-TADPOLE) setup[7]. Pump and probe pulses are non-collinearly focused on the sample and the transient transmission change $\Delta T/T$ is measured by a spectrometer[8].

To avoid degradation of the sample both low pump and probe fluences were used in the experiments, with spot sizes around 100 μm and energy in the 1 nJ range. Furthermore, we checked systematically that the low pump fluence ensured to stay in the linear regime. In order to preserve the short pulse duration of pump and probe pulses the colloidal suspension was contained in a 200-μm path length quartz cuvette.

## Electron and hole states in the CdTe nanorod

The energy levels in our CdTe nanorods were extracted by fitting the ground state absorption spectrum with a sum of five Gaussian curves whose parameters, of the first three given in the table below, are the energy of the excitonic transition (E [eV]), the linewidth ($\Gamma$ [eV]) and the oscillator strength (OS [a.u.]). The electronic levels of the excitonic transitions were then determined by band-structure calculations within the effective-mass approximation, while hole states were determined according to the 6-band model for valence band of CdTe.[9] $J_z$ gives the total angular momentum with the radial part of the orbital wave function differing by $\Delta m = 2$, i.e. being either ($m = J_z-1/2$, $m = J_z+3/2$) or ($m = J_z+1/2$, $m = J_z-3/2$). $m = 0$ states are labelled with $\Sigma$ while $m = \pm 1$ states are labelled with $\Pi$ (not relevant here) and $J_z$ gives the spin of the hole. The electron states have ½ spin. In Table 1 we report the calculated e-h transition energies in eV, by summing the bandgap for CdTe with the two energies of the electron and hole states, and correcting for large Coulomb interactions. For details the reader is referred to Ref. [10].

| Gaussian Fit (experiment) | | | Calculation | e - h transition | Assignment |
|---|---|---|---|---|---|
| E [eV] | $\Gamma$ [eV] | OS [a.u.] | E[eV] | | |
| 1.80 | 0.046 | 0.0026 | 1.79 | $\Sigma$ - $1\Sigma_{1/2}$ | **S1** |
| 1.87 | 0.080 | 0.0030 | 1.90 | $\Sigma$ - $1\Sigma_{3/2}$ | **S2** |
| | | | 1.96 | $\Sigma$ - $2\Sigma_{1/2}$ | **S2 or S3** |
| 2.07 | 0.152 | 0.010 | 2.03 | $\Sigma$ - $2\Sigma_{3/2}$ | **S3- $\Gamma$ point** |

**Table 1.** Values extracted from the Gaussian fits to the first three excitonic transitions in the experimental absorption spectrum of the CdTe nanorods: peak position (E[eV]), the broadening ($\Gamma$[eV]), and oscillator strength (OS [a.u.]). Calculated e-h transition energies in eV and their respective assignment according to the fit in the experimental spectrum.

## Model

The absorption cross section $\sigma_0(E)$ of the nanorod in the ground state is modeled as the overlap of broadened transitions, each described by a Gaussian function $G$:

$$\sigma_0(E) = \sum_{h,e} f_{h,e} G(E - E_{h,e}), \qquad (1)$$

where h describes the hole states, and e the electron states, $f_{h,e}$ is the transition strength, $E_{h,e}$ the transition energy. The differential absorption $\Delta\alpha$ can then be described by:

$$\Delta\alpha(E) = \sum_{h',e'} \delta n_{h',e'} \left(\sigma_0(E) - \sigma_{h',e'}(E)\right), \qquad (2)$$

where the h' and e' (hole and electron) depict the filled states and $\delta n_{h',e'}$ describes the volume density of excited nanorods. By assuming that the excited state level structure and the oscillator strengths are constant, then the absorption cross section of the excited system, $\sigma_{h',e'}(E)$, reflects small energy shifts (due to the population of higher excited states that induce renormalization of the energy levels) and the PB due to Pauli blocking of the occupied transitions h' and e':

$$\sigma_0(E) - \sigma_{h',e'}(E) = \sum_{h,e} f_{h,e} \left[ G(E - E_{h,e}) - G(E - E_{h,e} - \delta E_{h',e';h,e}) \right] +$$

$$\frac{1}{d_{e'}} \sum_{h \neq h'} f_{h,e'} G(E - E_{h,e'} - \delta E_{h',e';h,e'}) +$$

$$\frac{1}{d_{h'}} \sum_{e \neq e'} f_{h',e} G(E - E_{h',e} - \delta E_{h',e';h',e}) +$$

$$\left(\frac{1}{d_{e'}} + \frac{1}{d_{h'}}\right) f_{h',e'} G(E - E_{h',e'} - \delta E_{h',e';h',e'}), (3)$$

where $d_{h'}$ and $d_{e'}$ are the degeneracies of the $h'$ and $e'$ states. The first term of equation (3) gives the sum over the derivatives with energy shift $\delta E_{h',e';h,e}$ of the transition energy levels of the (h/h' → e/e') transition, which do not involve the filled states $h'$ and $e'$. Instead all other terms depict the sum of shifted transitions that are bleached due to Pauli blocking of states $h'$ and/or $e'$. For small energy shifts (with respect to the inhomogeneous broadening) we assume:

$$G(E - E_{h,e}) - G(E - E_{h,e} - \delta E_{h',e';h,e}) \cong \delta E_{h',e';h,e}\, G'(E - E_{h,e}) \quad (4)$$

and thus can express the differential absorption cross section as:

$$\Delta\alpha(E) \cong \sum_{n=1,4}(A_n\, G'_{\Gamma_{Sn}}(E - E_{Sn}) + B_n G_{\Gamma_{Sn}}(E - E_{Sn})) \quad (5)$$

Where An and Bn take into account the energy level shifts and PB, respectively. For details the reader is referred to Kriegel et al.[10].

Examples of the application of the model are reported for $t_2$=30 fs and $t_2$=500 fs in Fig. S2a and S2b, showing excellent agreement with the experimental data. Fig. S2c and d display the separate contributions of PB and shift; remarkably, strong derivative features arise at early times. Dynamics of the disentangled PB and shift terms are shown in Fig. S3. In particular, our model allows distinguishing an instantaneous rise of the shift of the S2 exciton (Fig. S3e) from a 50 fs build-up of its PB signal (Fig. S3b), reflecting carrier population dynamics. In contrast, this information is not directly accessible in the S3/S2 cross peak dynamics (Fig. 4b).
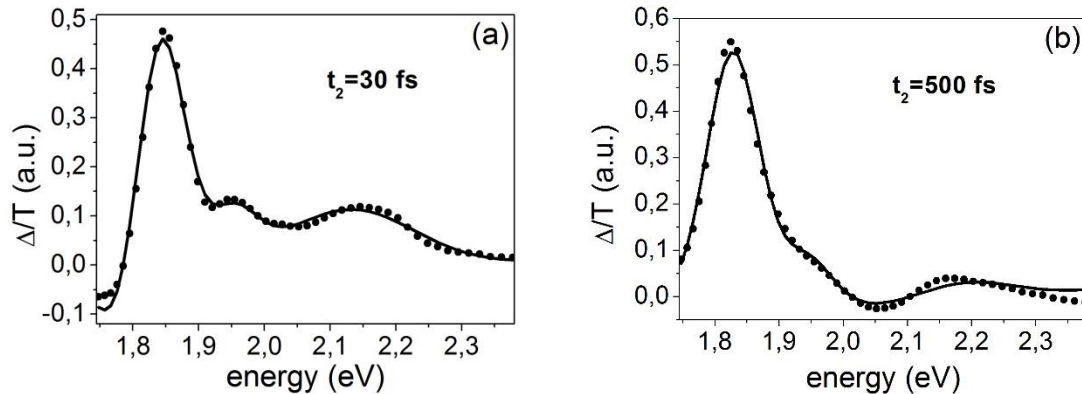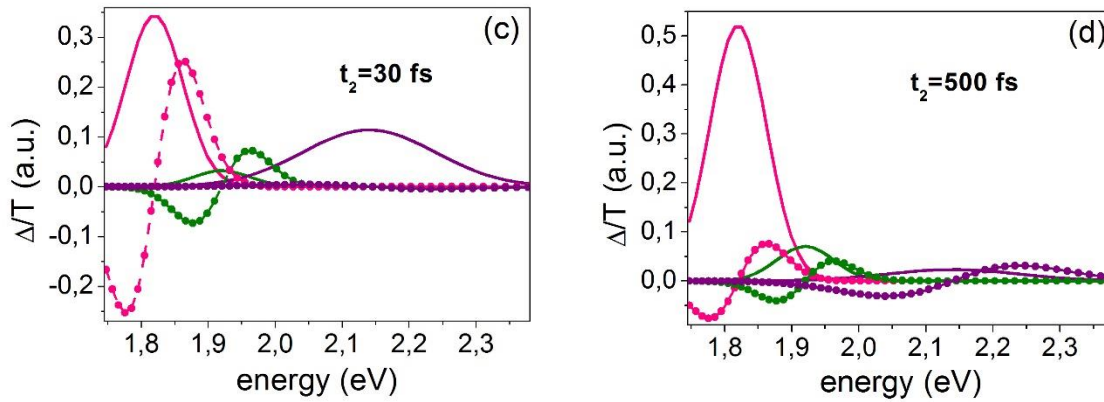
**Figure S2.** ΔT/T signal as a function of the detection energy for excitation fixed at 2.15 eV (S3): experimental data (points) corresponding to a horizontal cut of the 2DES maps in Fig. 2 and fits from the model (solid line), at $t_2$=30 fs (a) and $t_2$=500 fs (b). PB (solid line) and peak shift (dashed – points) contributions for the S1 (pink), S2 (green), S3 (purple) transitions at $t_2$=30 fs (c) and $t_2$=500 fs (d).
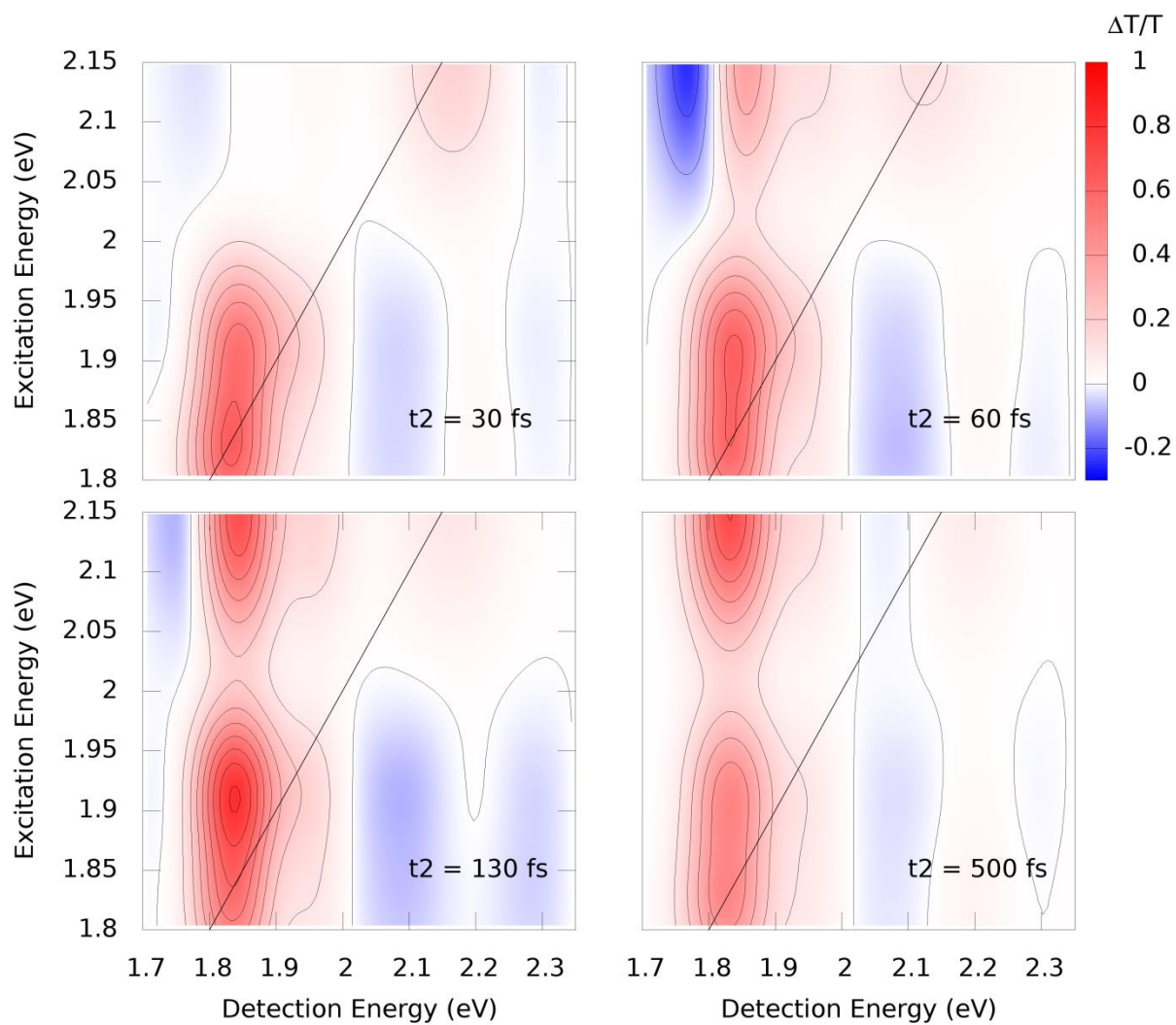
**Figure S3.** Fits of the 2DES maps at different $t_2$ delays using the model described above.
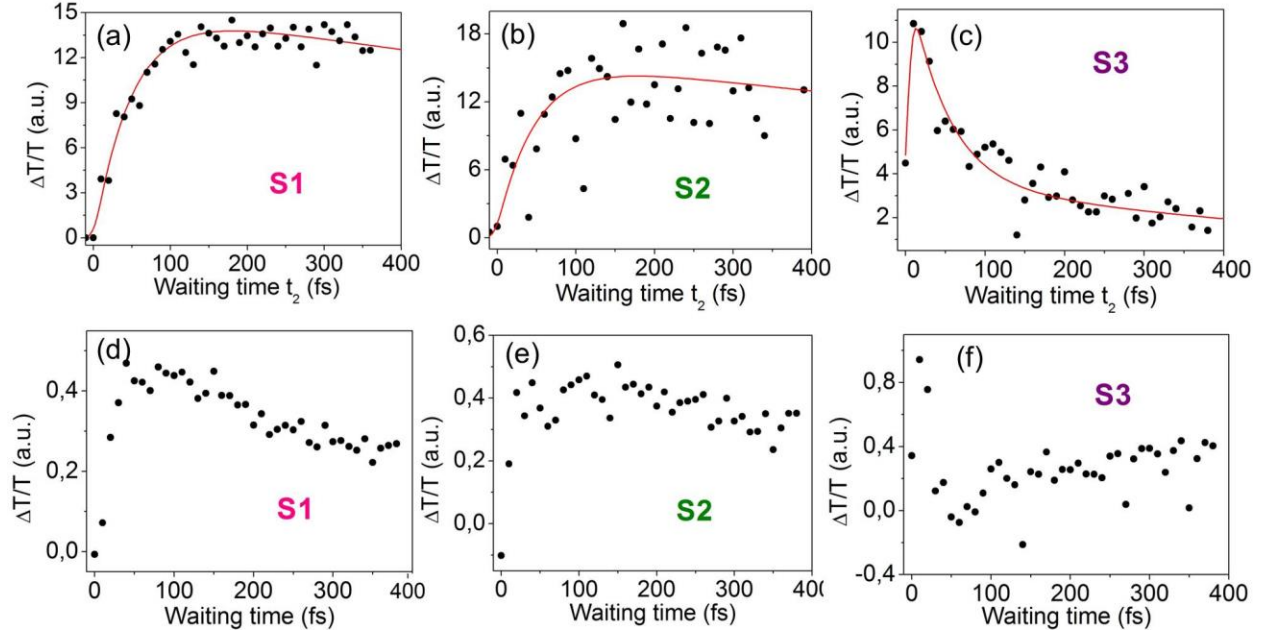
**Figure S4.** PB and peak shift dynamics obtained by the model explained in the text, for S1 (pink: a, d), S2 (green: b, e) and S3 (purple: c, f) exciton transitions, at 2.15 eV excitation energy (S3). PB dynamics were fitted with an exponential rise and a one or two-component exponential decay convoluted with the instrument response function.

## Fitting procedure

The dynamics of the S2/S2 and S3 diagonal peaks were fitted with bi-exponential decays:

$$S_{22/33}(t) = H(t)\left[C_{2/3}exp\left(-\frac{t}{\tau_{2/3}}\right) + C_r exp\left(-\frac{t}{\tau_r}\right)\right]$$

Where H(t) is the Heaviside function, $\tau_{2/3}$ are time constants corresponding to the fast relaxation processes out of S2/S3 and $\tau_r$ is a longer decay time constant.

The dynamics of the S2/S1 and S3/S1 cross peaks were fitted by a mono-exponential rise followed by a mono-exponential decay:

$$S_{21/31}(t) = H(t)\left[1 - exp\left(-\frac{t}{\tau_{2/3}}\right)\right]C_r exp\left(-\frac{t}{\tau_r}\right)$$

For all cases the fitting functions were convolved with the instrumental response function, corresponding to the autocorrelation of the excitation pulses, which was modeled as a Gaussian function.

REFERENCES

[1] Mukamel S., Principles of Nonlinear Optical Spectroscopy **1995**, Oxford University Press.

[2] Hamm P. and Zanni M. T., Concepts and Methods of 2D Infrared Spectroscopy **2011**, Cambridge University Press.

[3] A. M. Branczyk, Turner D. B. and Scholes G. D, Crossing Disciplines: A View on Two-Dimensional Optical Spectroscopy, *Ann. Phys.* **2014** *526(1-2)*, 31.

[4] Trebino R., Frequency-Resolved Optical Gating: The Measurement of Ultrashort Laser Pulses, **2000**, Springer.

[5] Réhault, J.; Maiuri, M.; Oriana, A.; Cerullo, G. Two-Dimensional Electronic Spectroscopy with Birefringent Wedges, *Rev. Sci. Instrum.* **2014** *85*, 123107.

[6] Brida, D.; Manzoni, C.; Cerullo, G. Phase-Locked Pulses for Two-Dimensional Spectroscopy by a Birefringent Delay Line, *Opt. Lett.* **2012** *37*, 3027-3029.

[7] Bowlan P., Gabolde P., Shreenath A., McGresham K., and Trebino R., Crossed-Beam Spectral Interferometry: a Simple, High-Spectral-Resolution Method for Completely Characterizing Complex Ultrashort Pulses in Real Time  *Opt. Express* **2006** *14*, 11892-11900.

[8] Polli D., Luer L., and Cerullo G., High-Time-Resolution Pump-Probe System with Broadband Detection for the Study of Time-Domain Vibrational Dynamics, *Rev. Sci. Instrum.* **2007** *78*, 103108.

[9] Shabaev, A.; Efros, A. L., 1D Exciton Spectroscopy of Semiconductor Nanorods, *Nano Lett.* **2004** *4*, 1821-1825.

[10] Kriegel, I.; Scotognella, F.; Soavi, G.; Brescia, R.; Rodrígez-Fernández, J.; Feldmann, J.; Lanzani, G.; Tassone, F. Delayed Electron Relaxation in CdTe Nanorods Studied by Spectral Analysis of the Ultrafast Transient Absorption, *Chem. Phys.* **2016** *471*, 39-45.